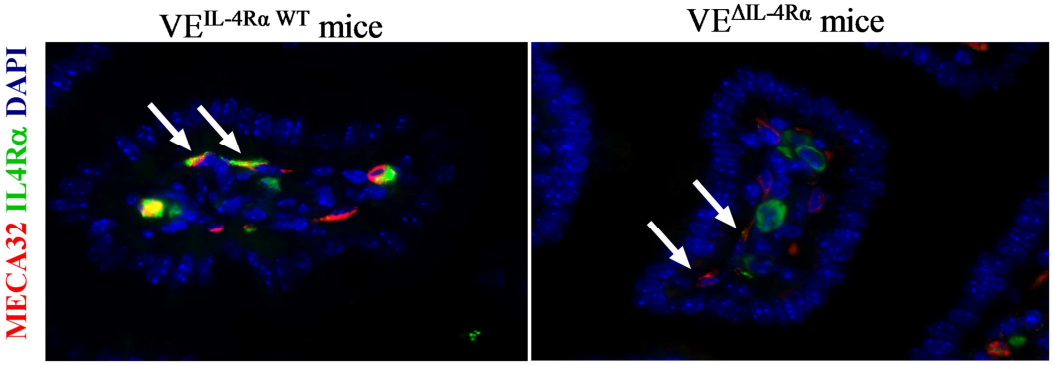

Yamani et al supp fig 1

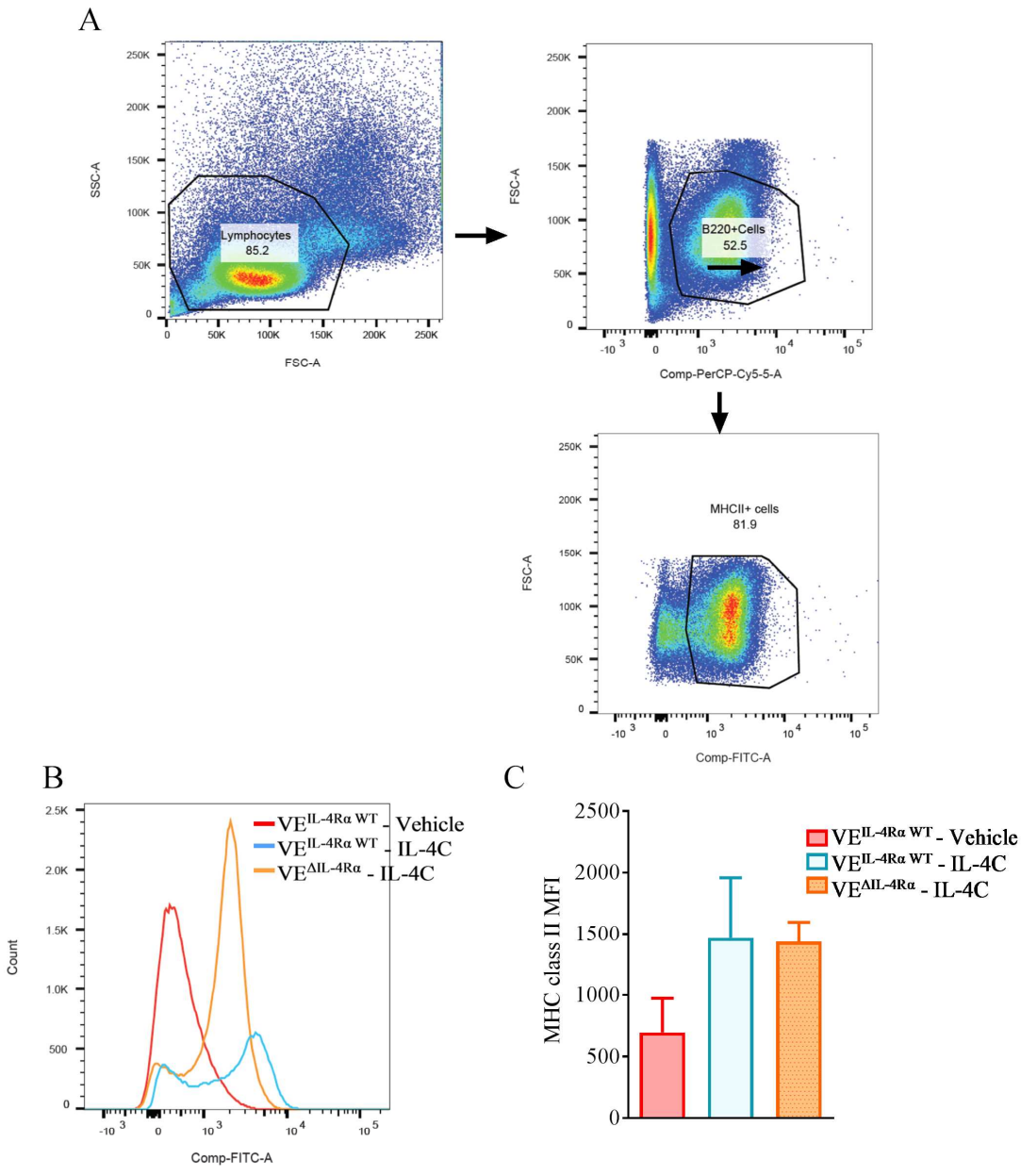

Yamani et al supp fig 2

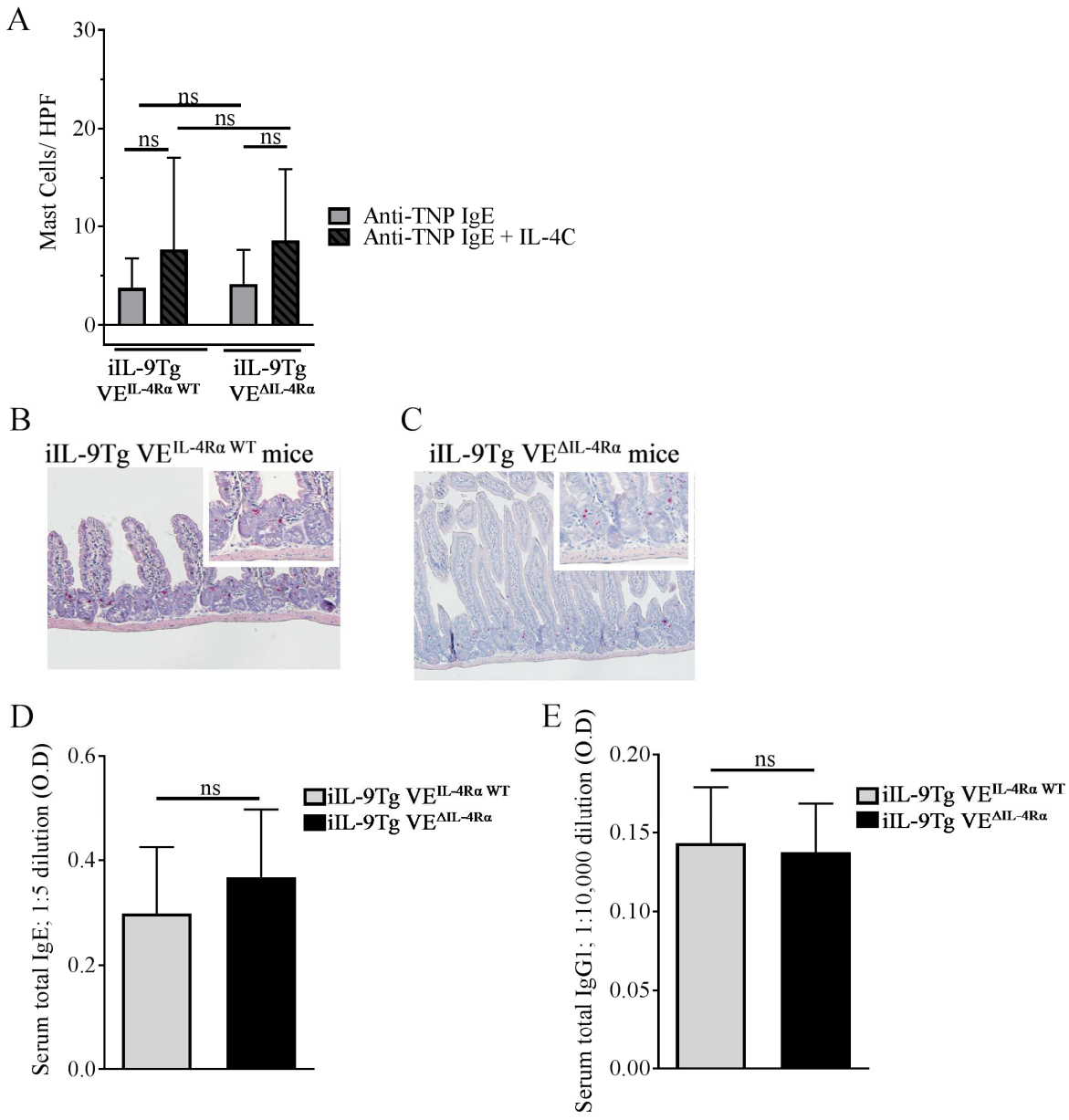

Yamani et al supp fig 3

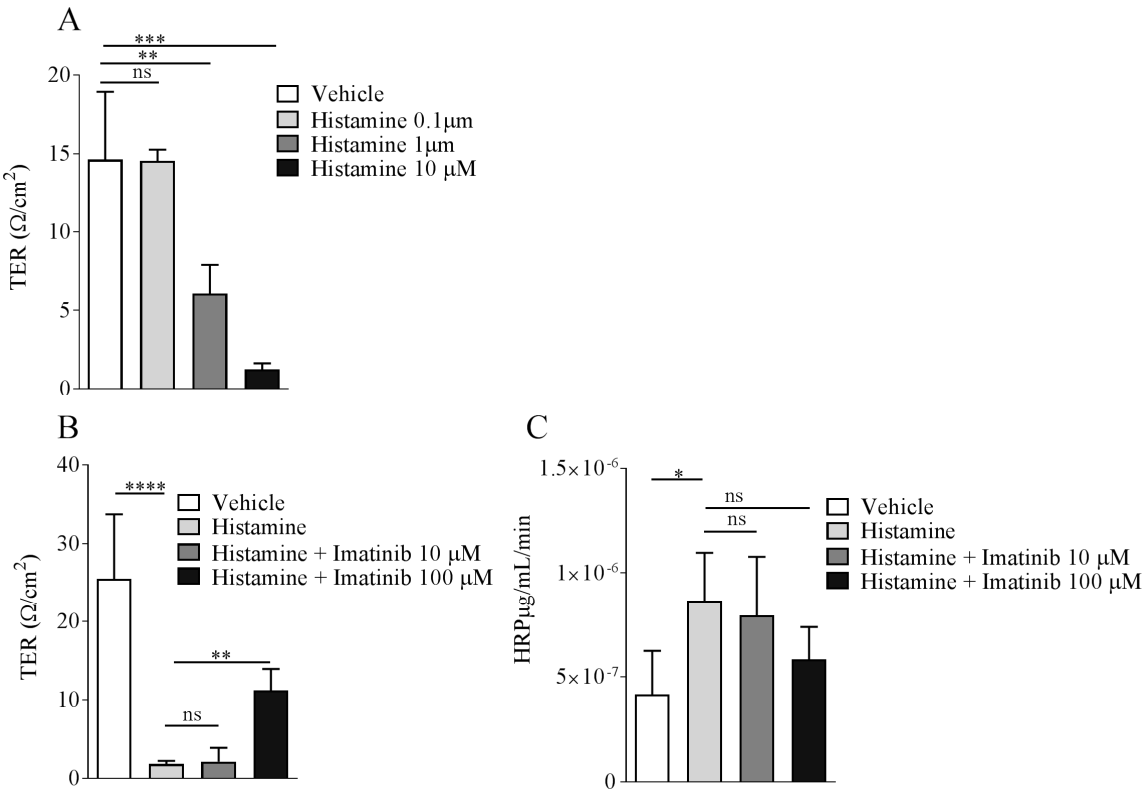

Yamani et al supp fig 4

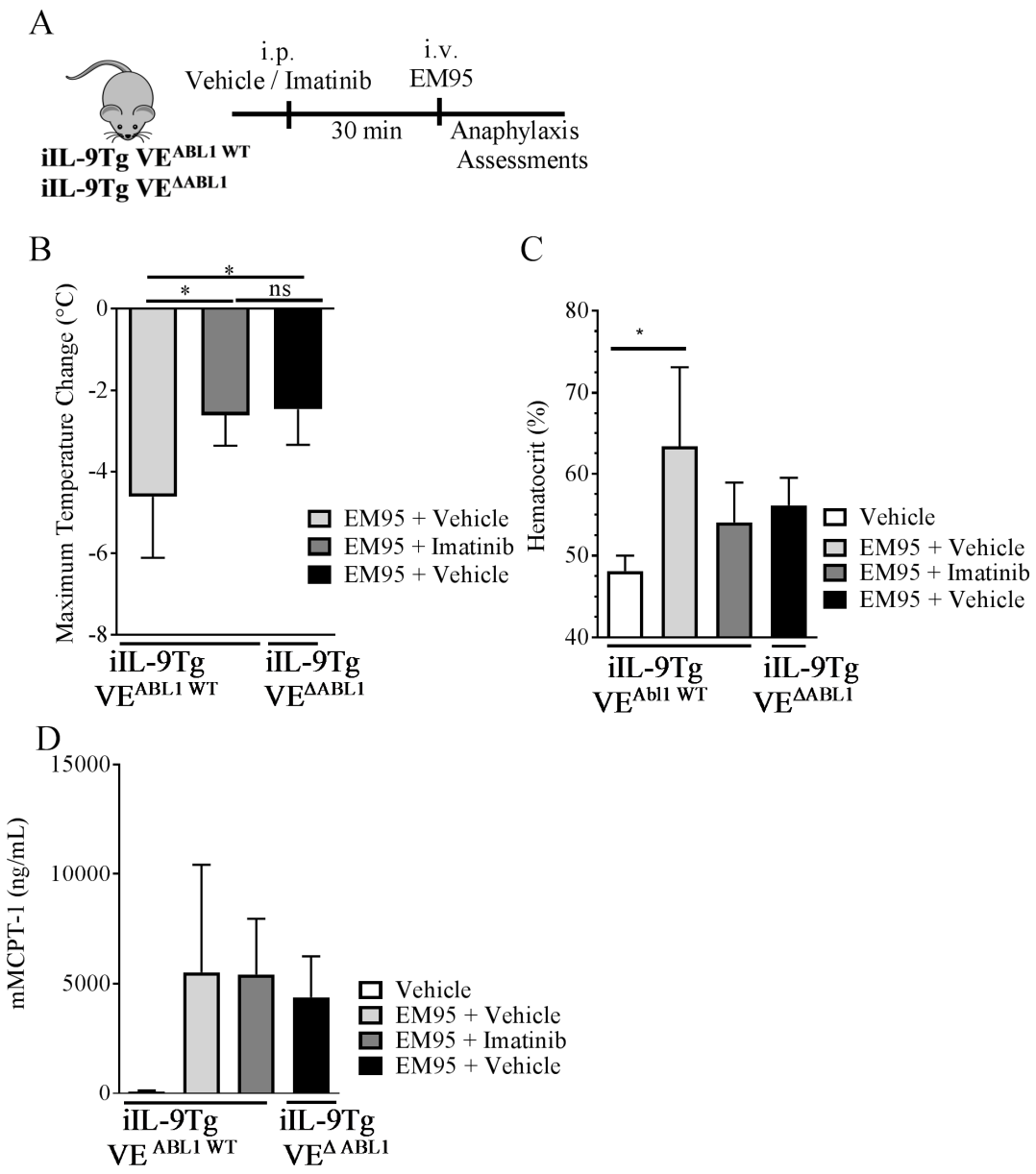

Yamani et al supp fig 5

Supplemental Figure Legends

Figure S1: VE$^{\Delta IL\text{-}4R\alpha}$ mice lack the expression of IL-4Rα chain on VE cells.
Immunofluorescence images of jejunum from VE IL-4Rα^{WT} and VE$^{\Delta IL\text{-}4R\alpha}$ mice. Anti- Panendothelial Cell Antigen staining with anti-rat monoclonal PLVAP antibody (MECA32) (red) identifies endothelial cells; anti-IL-4Rα staining (shown in green) was performed with anti–IL-4Rα (Santa Cruz, # sc-28361) and DAPI staining is shown in blue. White arrows show the presence of IL-4Rα chain staining on endothelial cells of VE IL-4Rα^{WT} mice and its absence on endothelial cells of VE$^{\Delta IL\text{-}4R\alpha}$ mice.

Figure S2: IL-4C is biologically active in the VE$^{\Delta IL\text{-}4R\alpha}$ mice.
Representative flow plots show the gating of the B220/MHC II population from lymphocytes (A). Histogram (B). Median florescence intensity (MFI) of FITC on PerCp/Cy5.5+ cells determined by flow cytometry (C). VE$^{IL\text{-}4R\alpha\ WT}$ and VE$^{\Delta IL\text{-}4R\alpha}$ mice were injected i.v. with vehicle or IL-4C (1 μg of IL-4 + 5 μg anti–IL-4 mAb). Mice were sacrificed the next day, and spleen cells were stained with anti-mouse MHC II (I-A), FITC, and anti-mouse/human CD45R/B220 PerCP/Cy5.5^{+} antibody. Data are represented as the mean ± SD; = 2 mice per group from n = 1 experiment.

Figure S3: The effect of vascular endothelial IL-4Rα chain on hypovolemic shock is mast cell and immunoglobulin independent.
Intestinal MC counts (A), photomicrograph of CAE-stained intestinal section of iIL-9Tg VE$^{IL\text{-}4R\alpha\ WT}$ (B) and iIL-9Tg VE$^{\Delta IL\text{-}4R\alpha}$ (C), serum Total serum IgE (D). Total serum IgG1 (E) of iIL-9Tg VE$^{IL\text{-}4R\alpha\ WT}$ and iIL-9Tg VE$^{\Delta IL\text{-}4R\alpha}$ mice following treatment with anti-TNP IgE and with IL-4C or vehicle and with TNP-OVA. Serum was collected from untreated iIL-9Tg VE$^{IL\text{-}4R\alpha\ WT}$ and iIL-9Tg VE$^{\Delta IL\text{-}4R\alpha}$ mice. Data are represented as the as the mean ± SD; n = 4-5 mice per group (A, D-E). Photomicrograph 10X magnification; insert, 40X magnifications (B-C). ns > 0.05.

Figure S4: Histamine-induced VE-permeability in EA.hy926 cells is inhibited by Imatinib.
(A) Confluent monolayers of cell line EA.hy 296 (EVOM >100 ohms) were mounted in Ussing chambers and stimulated with different doses of histamine (0.1 – 10μM) for 30 min and TER was determined using Ohms law. EA.hy 296 cells were pretreated with different dose of imatinib (0 – 100μM) for 3 h, mounted in Ussing Chambers and treated with histamine (100 μM for 30 min) and TER (B) and HRP flux (C) was determined. Data are represented as the as the mean ± SD; n = 3 wells per group. **** P < 0.0001, *** P < 0.001, ** P < 0.01, * P < 0.05, ns > 0.05.

Figure S5: Hypovolemic shock induced by EM95 is dependent on VE ABL1.
Experimental regimen (A), Maximum temperature change (B), Hematocrit percentage (C), and mMCPT-1 (D) in iIL-9Tg VE$^{\Delta ABL1}$ (iIL-9^{WT} Tie2^{cre} ABL1$^{fl/fl}$) and iIL-9Tg VE$^{ABL1\ WT}$ (iIL-9^{WT} Tie2^{WT} Abl1$^{fl/fl}$; used as a WT control.) i.p. treated

with vehicle or imatinib (1.25 mg/mice) 30 min before EM95 (i.v. 2 mg / 200 mL). iIL-9Tg VE$^{\Delta Abl1}$ received EM95 only. Data are represented as the mean ± SD; n = 4-6 mice per group from n = 3 experiments. * $P < 0.05$, ns > 0.05.